Check for updates

International Journal of Cancer

WILEY | UICC

RESEARCH ARTICLE OPEN ACCESS

Tumor Markers and Signatures

Pretreatment EBV-DNA/TLG-Based Risk Stratification Is Associated With Survival Outcomes in Nonmetastatic Nasopharyngeal Carcinoma: An Exploratory Study

Mehmet Çağrı Duymaz[1] | Ece Özkaya Duymaz[1] | Nazlı Ünsal[2] | Recep Bekiş[2] | Büşra Tozduman[3] | Özgür Appak[4] | Ayşe Demiral[1] | Oğuz Çetinayak[1]

[1]Department of Radiation Oncology, Dokuz Eylül University Faculty of Medicine, Izmir, Türkiye | [2]Department of Nuclear Medicine, Dokuz Eylül University Faculty of Medicine, Izmir, Türkiye | [3]Department of Public Health, Dokuz Eylül University Faculty of Medicine, Izmir, Türkiye | [4]Department of Medical Microbiology, Dokuz Eylül University Faculty of Medicine, Izmir, Türkiye

Correspondence: Ece Özkaya Duymaz (ece.ozkaya@deu.edu.tr) | Mehmet Çağrı Duymaz (mehmetcagri.duymaz@deu.edu.tr)

Received: 14 April 2026 | **Revised:** 12 August 2026 | **Accepted:** 24 August 2026

Keywords: Epstein–Barr virus DNA | nasopharyngeal carcinoma | PET/CT | prognosis | total lesion glycolysis

ABSTRACT

Whether combining pretreatment plasma Epstein–Barr virus DNA (EBV-DNA) with 18F-FDG PET/CT-derived total lesion glycolysis (TLG) improves prognostic stratification in nonmetastatic nasopharyngeal carcinoma (NPC) is unclear, particularly in nonendemic populations. We retrospectively analyzed 86 eligible nonmetastatic NPC patients treated with definitive radiotherapy (2010–2024) at a single nonendemic-region institution. EBV-DNA (prespecified cutoff 3500 copies/mL) and TLG (cutoff 200, ROC-derived within this cohort) were dichotomized. Both were available in 59/86 patients (68.6%), who differed from the rest in nodal and overall stage and in RT technique. Baseline PET/CT was in-house in 57 of 86 patients, and a robustness analysis in that subgroup is reported. Given limited events (13 PFS, 9 OS), Cox analyses are exploratory and were supplemented with penalized regression and bootstrap validation. At a median follow-up of 75.5 months, 5-year PFS and OS for the whole cohort ($n = 86$) were 81.1% and 85.9%. The EBV-DNA$_{high}$/TLG$_{high}$ subgroup remained associated with inferior PFS after adjustment in an exploratory model (adjusted HR = 3.97, 95% CI: 1.32–11.93) and, in a single-variable model, with inferior OS (HR = 4.13, 95% CI: 1.10–15.52). Discrimination was comparable to the individual-biomarker model for PFS and lower for OS. Five-year PFS fell monotonically across the four risk groups in the complete-case cohort ($n = 59$; 89.7%–58.3%). OS differed across groups (log-rank $p = 0.044$) but was not strictly monotonic, with wide, overlapping confidence intervals. This two-biomarker model is hypothesis-generating and needs prospective, multicenter validation before any consideration of risk-adapted treatment.

Abbreviations: 3D-CRT, three-dimensional conformal radiotherapy; AIC, Akaike information criterion; AJCC, American Joint Committee on Cancer; AUC, area under the curve; CI, confidence interval; CTV, clinical target volume; EBV, Epstein–Barr virus; EBV-DNA, Epstein–Barr virus deoxyribonucleic acid; FDG, fluorodeoxyglucose; GTV, gross tumor volume; HR, hazard ratio; IMRT, intensity-modulated radiotherapy; KPS, Karnofsky Performance Status; LLOD, lower limit of detection; MTV, metabolic tumor volume; NPC, nasopharyngeal carcinoma; OAR, organ at risk; OS, overall survival; PET/CT, positron emission tomography/computed tomography; PFS, progression-free survival; PTV, planning target volume; qPCR, quantitative polymerase chain reaction; ROC, receiver operating characteristic; RT, radiotherapy; SIB, simultaneous integrated boost; STROBE, Strengthening the Reporting of Observational Studies in Epidemiology; SUV, standardized uptake value; TLG, total lesion glycolysis; UICC, Union for International Cancer Control; VMAT, volumetric modulated arc therapy; VOI, volume of interest; WHO, World Health Organization.

This study was presented as a Poster Highlight (poster number: E26-2147) at the ESTRO 2026 Congress, held on 15–19 May 2026 in Stockholm, Sweden.

This is an open access article under the terms of the Creative Commons Attribution License, which permits use, distribution and reproduction in any medium, provided the original work is properly cited.

© 2026 The Author(s). *International Journal of Cancer* published by John Wiley & Sons Ltd on behalf of UICC.

What's New?

Prognostic assessment for nonmetastatic nasopharyngeal carcinoma (NPC) relies on standardized staging, which is based on anatomical tumor spread. Patients within the same stage, however, can have dramatically different outcomes. The present study applied an experimental model to assess the prognostic value of plasma Epstein–Barr virus (EBV) DNA combined with total lesion glycolysis (TLG) in radiotherapy-treated nonmetastatic NPC patients. The model revealed a subgroup of patients with high EBV DNA and high TLG who experienced significantly reduced survival. Outcome discrimination, however, was similar to either marker alone. Model refinement and validation are necessary to better capture biological heterogeneity in nonmetastatic NPC.

1 | Introduction

Nasopharyngeal carcinoma (NPC) shows an uneven geographic distribution, with most of the 120,000 new cases and 73,000 deaths estimated by GLOBOCAN 2022 occurring in Asia, particularly Southern China and Southeast Asia [1–5]. In endemic regions, the nonkeratinizing histological subtype predominates and is strongly associated with latent Epstein–Barr virus (EBV) infection, which is central to NPC pathogenesis [1, 2, 6].

Radiotherapy, with or without cisplatin-based systemic therapy, remains the cornerstone of curative treatment for nonmetastatic NPC [1, 6, 7]. Advances in IMRT/VMAT and the integration of induction and concurrent chemotherapy have improved outcomes, yet a proportion of patients with locoregionally advanced disease still experience recurrence; better prognostic stratification is therefore needed [6, 8].

The AJCC/UICC TNM staging system remains the principal framework for prognostic assessment in NPC [9], but because it is based solely on anatomical extent, it does not capture biological heterogeneity, and patients within the same stage can have markedly different outcomes [10, 11]. Pretreatment plasma EBV-DNA is among the most extensively validated complementary biomarkers, with elevated levels consistently associated with greater tumor burden and inferior PFS/OS across retrospective, prospective, and meta-analytic data [12–17]; inter-assay variability and the lack of a universal cutoff remain barriers to standardization [13, 18].

In parallel, ^{18}F-FDG PET/CT-derived volumetric parameters, metabolic tumor volume (MTV) and total lesion glycolysis (TLG, the product of MTV and SUVmean [19]), have gained attention as prognostic biomarkers, integrating metabolic activity with lesion volume [20–24]. Standardized segmentation and thresholds remain unestablished, limiting routine clinical use [22, 25].

EBV-DNA and TLG may reflect partly overlapping aspects of disease burden, circulating viral–tumoral load and imaging-derived metabolic extent [26, 27]. Combining them may improve discrimination beyond either marker alone [26, 28, 29], but a combined pretreatment EBV-DNA/TLG model remains underexplored in nonmetastatic NPC, especially in nonendemic populations. We therefore investigated the combined prognostic value of both markers in an eligible nonmetastatic NPC cohort treated with definitive radiotherapy at a single nonendemic-region institution.

2 | Materials and Methods

2.1 | Study Design, Patients, and Patient Flow

A total of 120 consecutive patients with histologically confirmed nasopharyngeal carcinoma were screened from institutional treatment records between January 2010 and January 2024. Five patients with de novo metastatic disease were excluded. Of the remaining 115, 17 were excluded for no pretreatment PET/CT and 12 because PET/CT was performed externally and the original imaging data needed for standardized quantitative analysis were unavailable. The remaining 86 patients, all with accessible pretreatment PET/CT and completed definitive curative-intent radiotherapy, formed the overall study cohort (Figure 1). The study followed STROBE guidelines.

Pretreatment plasma EBV-DNA was available for 66 of the 86 patients. TLG could be reliably quantified in 76; in the other 10, image quality, missing reconstruction information, or uncertain lesion boundaries made quantification unreliable. Both measures were available in 59 patients, who formed the complete-case cohort for the combined biomarker analyses. Among the 27 patients lacking one or both, TLG alone was available in 17, EBV-DNA alone in 7, and neither in 3.

Pretreatment PET/CT and EBV-DNA testing were both performed as part of routine clinical care, not under a prospective protocol. Cohort-level reasons for a missing scan or unobtainable source imaging are given above. The patient-level reason an individual EBV-DNA measurement was not obtained was not documented and could not be reconstructed, so this missing-data mechanism cannot be assumed to be random. We therefore compared the complete-case and noncomplete-case cohorts. The complete-case cohort differed from the 27 noncomplete-case patients in nodal classification, overall stage, and RT technique (Table S1), consistent with both tests being used preferentially in more recently treated, more advanced-stage, VMAT-treated patients. A VMAT-only sensitivity analysis partly addresses this enrichment (Limitations).

2.2 | Imaging, Radiotherapy, and Systemic Therapy

Pretreatment staging used ^{18}F-FDG PET/CT and/or contrast-enhanced head-and-neck MRI, supplemented by thorax–abdomen CT when indicated, reviewed by a multidisciplinary tumor board and staged per UICC/AJCC TNM 8th edition. Patients were simulated supine with thermoplastic immobilization; the planning CT was fused with diagnostic MRI (and PET/CT when appropriate) before contouring GTV/CTV/PTV per contemporary NPC target delineation principles.

Definitive radiotherapy was delivered predominantly with VMAT (81.4%) using simultaneous integrated boost (69/60/54 Gy to high-/intermediate-/low-risk volumes); 3D-CRT (18.6%) was used in a minority of patients treated before 2014, to a total

10970215, 0, Downloaded from https://onlinelibrary.wiley.com/doi/10.1002/ijc.70732 by Mehmet Çar Duymaz - Dokuz Eylul University , Wiley Online Library on [02/09/2026]. See the Terms and Conditions (https://onlinelibrary.wiley.com/terms-and-conditions) on Wiley Online Library for rules of use; OA articles are governed by the applicable Creative Commons License

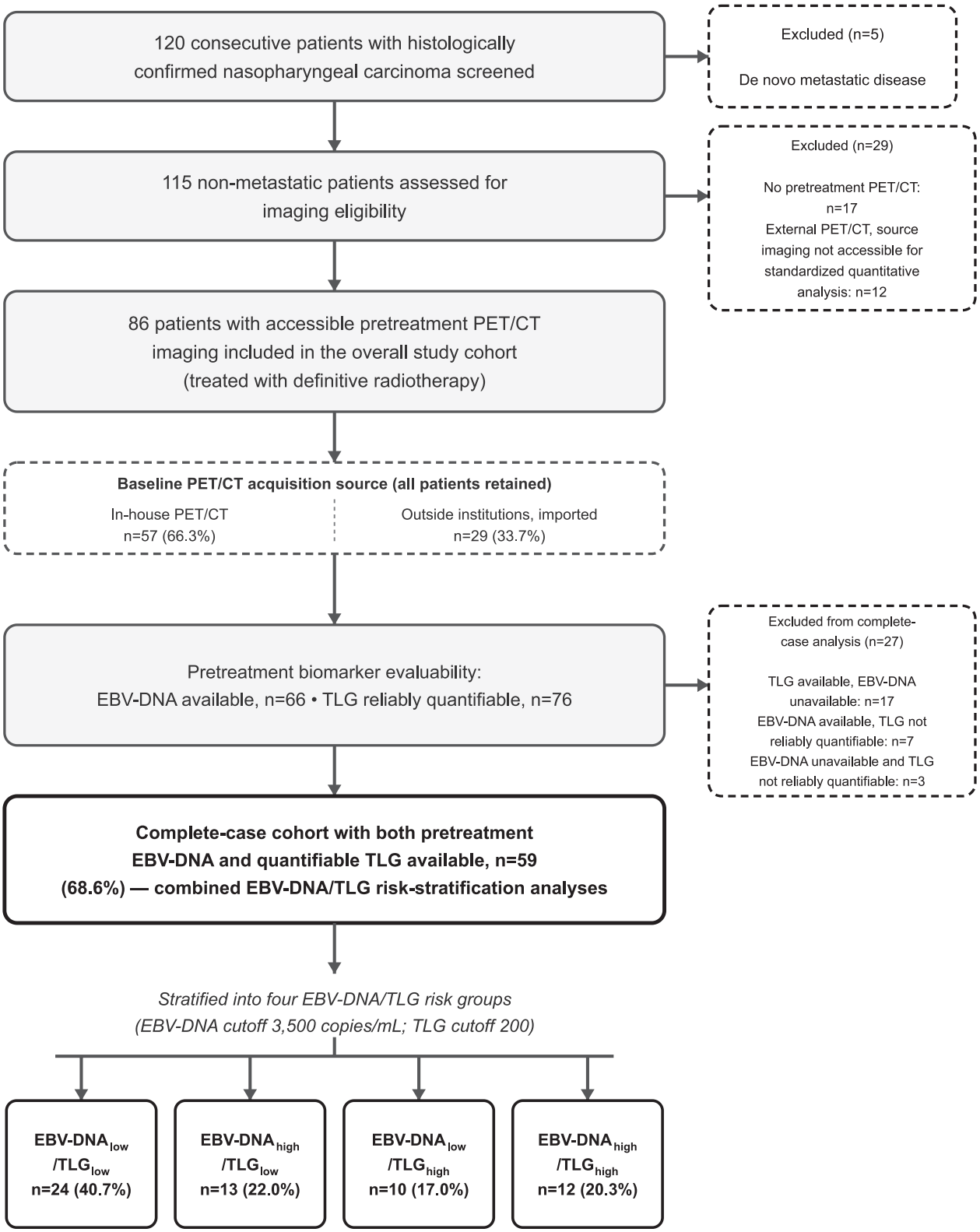

FIGURE 1 | STROBE-style patient-selection flow diagram. Flow of the 120 consecutive patients with histologically confirmed nasopharyngeal carcinoma screened. Exclusions were de novo metastatic disease ($n = 5$) and imaging ineligibility (no pretreatment PET/CT, $n = 17$; externally acquired PET/CT without accessible source imaging, $n = 12$), leaving the 86-patient overall study cohort. The diagram then shows biomarker availability and inclusion in the complete-case EBV-DNA/TLG analysis. Within the 86-patient overall cohort, baseline PET/CT was performed in-house in 57 patients and at outside institutions in 29; source images were obtained and re-analyzed centrally.

dose of 70 Gy in two phases. RT duration (first-to-last fraction) was recorded, with ≤49 days as the higher-hazard comparator (Statistical Analysis).

Concurrent chemotherapy consisted predominantly of cisplatin administered either weekly at 40 mg/m^2 or every 3 weeks at 100 mg/m^2. Carboplatin was used in patients considered

10970215, 0, Downloaded from https://onlinelibrary.wiley.com/doi/10.1002/ijc.70732 by Mehmet Çar Duymaz - Dokuz Eylul University , Wiley Online Library on [02/09/2026]. See the Terms and Conditions (https://onlinelibrary.wiley.com/terms-and-conditions) on Wiley Online Library for rules of use; OA articles are governed by the applicable Creative Commons License

unsuitable for continued cisplatin treatment. Induction chemotherapy regimens and their frequencies are summarized in Table 1. Cumulative cisplatin dose could not be reliably reconstructed for all patients because of incomplete retrospective documentation, and chemotherapy dose reductions and omitted cycles, as distinct from radiotherapy interruptions, were not systematically documented.

2.3 | Plasma EBV-DNA and PET/CT-Derived TLG

Plasma EBV-DNA testing was performed in the institutional molecular diagnostics laboratory as part of routine clinical practice. Peripheral blood was drawn during initial staging, before any anticancer treatment including induction chemotherapy and radiotherapy, so all measurements represent true pretreatment values. DNA was extracted with the QIAsymphony SP system (QIAGEN, Hilden, Germany), and EBV-DNA was quantified with the artus EBV RG PCR Kit (QIAGEN) on the Rotor-Gene Q real-time PCR platform. Per the manufacturer, the assay amplifies a 97-bp region of the EBV genome; the exact locus and the proprietary primer/probe sequences are not disclosed. The reported analytical detection limit is 1.02 copies/μL of eluate, corresponding to a 95% probability of detection. A separately validated lower limit of quantification was not specified by the manufacturer and was not available from institutional laboratory records. Internal, positive, and negative controls were included in each run, and results were interpreted as recommended by the manufacturer. Samples with no EBV-specific amplification but a valid internal-control signal were classified as undetectable and assigned 0 copies/mL. Intervals between collection, plasma processing, and analysis were not systematically recorded, again because testing was routine rather than protocol-driven. The extraction platform, PCR kit, instrument, and interpretation protocol were unchanged throughout the study period.

Baseline ^{18}F-FDG PET/CT examinations performed for initial staging between 2010 and 2024 were retrieved in DICOM format. Of the 86 baseline examinations, 57 (66.3%) were performed in-house and retrieved from the institutional nuclear medicine PACS archive; all in-house examinations were acquired on a single PET/CT scanner, which remained unchanged throughout the study period. The remaining 29 examinations (33.7%) were performed at outside institutions and imported into DICOM format from the referring centers. Baseline imaging across the cohort as a whole was therefore not acquired on a single standardized system. Owing to the retrospective design and the inclusion of examinations acquired at different institutions, no dedicated cross-scanner harmonization procedure was applied. The corresponding acquisition parameters were not uniformly available for externally performed examinations.

In-house examinations were acquired on a single combined PET/CT scanner (Philips Gemini TF) in three-dimensional mode. After patient preparation, including fasting for at least 4–6 h and confirmation of a blood glucose concentration below 200 mg/dL, each patient received an intravenous injection of ^{18}F-FDG. The average administered dose was 0.11 (0.10–0.12) mCi/kg [4.1 (3.7–4.4) MBq/kg]. Images were acquired approximately 60 (50–70) minutes after tracer administration, with a voxel size of 4 × 4 × 4 mm. Emission images were obtained from the skull base to the mid-thigh, with 10–12 bed positions per patient and an acquisition time of 1.5 min per bed position. Transmission images were acquired by low-dose CT (50 mA, 120 kVp, pitch 5 mm). Images were reconstructed with the row-action maximum-likelihood algorithm.

All examinations, including externally acquired ones, were analyzed centrally by a single nuclear medicine physician with 4 years of PET/CT reporting experience, using identical methodology and LIFEx (v25.06.1; www.lifexsoft.org). The primary nasopharyngeal tumor and all FDG-avid cervical lymph nodes were segmented with a 40% SUVmax threshold, with manual adjustment of the volumes of interest (VOIs) where needed. A relative rather than absolute SUV threshold was used because it may reduce, but does not eliminate, inter-scanner variability. Where cervical nodes were equivocal, metastatic involvement was confirmed against available histopathology. For each VOI we recorded metabolic tumor volume (MTV), SUVmax, and SUVmean; lesion TLG was MTV × SUVmean, and total locoregional TLG was the sum of TLG for the primary tumor and metastatic cervical nodes. Because segmentation covered the primary tumor and cervical nodal disease rather than all metabolically active lesions body-wide, this parameter is called total locoregional TLG throughout. Inter-observer reproducibility was not formally assessed.

The EBV-DNA cutoff (3500 copies/mL) was prespecified in the prior literature to limit overfitting before outcome analyses. Because no standardized TLG threshold exists, the TLG cutoff was derived within this cohort by ROC analysis for a composite PFS event ($n = 76$; AUC = 0.656; Youden-optimal threshold 196.5, rounded to 200). A cumulative/dynamic IPCW time-dependent ROC analysis for the 5-year PFS endpoint in the same cohort yielded a closely similar cut-point (AUC = 0.656; 195.9). Because both analyses share the same cohort, this is not independent validation, and the TLG = 200 threshold remains provisional. Patients were classified into four groups (EBV-DNA$_{low}$/TLG$_{low}$, EBV-DNA$_{high}$/TLG$_{low}$, EBV-DNA$_{low}$/TLG$_{high}$, EBV-DNA$_{high}$/TLG$_{high}$); analyses also compared EBV-DNA$_{high}$/TLG$_{high}$ versus all remaining patients.

2.4 | Follow-Up, Endpoints, and Statistical Analysis

Response was assessed 3 months postradiotherapy (RECIST 1.1); patients were followed every 3 months (years: 1–2), every 6 months (years: 3–5), then annually. PFS and OS were both calculated from the start of treatment, applied uniformly to every patient. The start of treatment was the start of induction chemotherapy for patients who received it, and otherwise the start of definitive radiotherapy. The primary endpoint was PFS (time to local, regional, or distant progression, or death from any cause); the secondary endpoint was OS (time to death from any cause). Patients free of the relevant event were censored at the date of last follow-up. Median follow-up was estimated using the reverse Kaplan–Meier method. Descriptive 5-year Kaplan–Meier estimates for the whole cohort used all 86 patients; all Kaplan–Meier 95% confidence intervals reported here and in Table 3 were computed on the complementary log–log (log–log) scale. The

10970215, 0, Downloaded from https://onlinelibrary.wiley.com/doi/10.1002/ijc.70732 by Mehmet Çar Duymaz - Dokuz Eylul University , Wiley Online Library on [02/09/2026]. See the Terms and Conditions (https://onlinelibrary.wiley.com/terms-and-conditions) on Wiley Online Library for rules of use; OA articles are governed by the applicable Creative Commons License

TABLE 1 | Baseline patient and treatment characteristics ($n = 86$).

Variable	Category	Value
Age (years)	—	49 (12–76)
Age subgroup	≤ 15 years	7 (8.1%)
Sex	Male	67 (77.9%)
	Female	19 (22.1%)
KPS	≥ 90	84 (97.7%)
	< 90	2 (2.3%)
Smoking history	Yes	42 (48.8%)
	No	44 (51.2%)
WHO histology	Nonkeratinizing undifferentiated	80 (93.0%)
	Other (5 keratinizing SCC, 1 nonkeratinizing differentiated)	6 (7.0%)
T classification	T1	22 (25.6%)
	T2	35 (40.7%)
	T3	12 (14.0%)
	T4	17 (19.8%)
N classification	N0	9 (10.5%)
	N1	15 (17.4%)
	N2	37 (43.0%)
	N3	25 (29.1%)
Overall stage (AJCC 8th)	I–II	17 (19.8%)
	III	28 (32.6%)
	IVA	41 (47.7%)
Pretreatment EBV-DNA (copies/mL)	—	1857.5 (0–544,380); $n = 66$ available
TLG	—	156.4 (22.6–955.2); $n = 76$ available
Both biomarkers available (complete-case)	—	59 (68.6%)
Biomarker gaps: EBV-DNA missing (TLG quantifiable)/TLG not quantifiable (EBV-DNA available)/neither available	—	17/7/3
Diagnosis era	2010–2016	36 (41.9%)
	2017–2024	50 (58.1%)
RT technique	VMAT	70 (81.4%)
	3D-CRT	16 (18.6%)
RT dose (Gy)	—	69 (66–70)
RT interruption (≥ 1 day)	Yes	4 (4.7%)
Neoadjuvant chemotherapy	Yes	30 (34.9%)

(Continues)

10970215, 0, Downloaded from https://onlinelibrary.wiley.com/doi/10.1002/ijc.70732 by Mehmet Çar Duymaz - Dokuz Eylul University , Wiley Online Library on [02/09/2026]. See the Terms and Conditions (https://onlinelibrary.wiley.com/terms-and-conditions) on Wiley Online Library for rules of use; OA articles are governed by the applicable Creative Commons License

TABLE 1 | (Continued)

Variable	Category	Value
Regimen (of those treated)	Gemcitabine + cisplatin	13/30 (43.3%)
	DCF/triple combination (docetaxel + cisplatin + 5-FU)	11/30 (36.7%)
	Docetaxel + cisplatin (doublet)	3/30 (10.0%)
	5-FU + cisplatin (doublet)	1/30 (3.3%)
	Other (cisplatin + etoposide or unspecified modified regimen)	2/30 (6.7%)
Concurrent chemotherapy	Yes	75 (87.2%)
Agent (of those treated)	Cisplatin alone	70/75 (93.3%)
	Carboplatin alone	4/75 (5.3%)
	Cisplatin and carboplatin (sequential)	1/75 (1.3%)

Note: Data are presented as *n* (%) for categorical variables and median (range) for continuous variables. Interruption duration was available for three of the four patients with a radiotherapy interruption (2, 2, and 4 days). Full univariate Cox regression results for PFS/OS are in Table S2.
Abbreviations: 3D-CRT, three-dimensional conformal radiotherapy; AJCC, American Joint Committee on Cancer; EBV-DNA, Epstein–Barr virus deoxyribonucleic acid; KPS, Karnofsky Performance Status; RT, radiotherapy; TLG, total lesion glycolysis; VMAT, volumetric modulated arc therapy; WHO, World Health Organization.

four-group EBV-DNA/TLG comparisons and the four primary Cox models reported in Table 2 used the 59-patient complete-case cohort. Available-case, continuous-variable, and in-house robustness analyses used the relevant populations specified in the Supporting Information. Because of limited events (13 PFS, 9 OS), the principal univariate and adjusted Cox analyses are presented as exploratory throughout.

Given the limited event-to-covariate ratio, analyses were supplemented with penalized (ridge, fixed penalty) Cox regression, bootstrap-based (1000 resamples, Harrell's method) optimism-corrected C-indices, and nonnested model-comparison metrics (C-index, AIC) between the individual-biomarker and composite-biomarker models. Calibration plots and decision-curve analysis were not performed, because 9–13 events per model would yield unstable and potentially misleading estimates (Supplementary Methods). TLG and log-EBV-DNA were also modeled as continuous variables and with natural cubic splines (3 df) to test linearity. The proportional-hazards assumption was assessed for all four primary Table 2 models by Schoenfeld residual testing. Motivated by the visual separation in the Kaplan–Meier curves, we additionally fit a post hoc piecewise Cox model (split at 30 months) and a covariate-by-log[time] interaction term. Sensitivity analyses restricted the complete-case cohort to VMAT-treated patients, excluded the three complete-case patients aged ≤15 years, and repeated the OS analysis in available-case populations; a further robustness analysis restricted the cohort to the patients whose baseline PET/CT was acquired in-house (Table S7). Detailed information on penalized Cox regression and bootstrap-based internal validation, as well as model-comparison metrics, continuous-variable and natural cubic spline analyses, proportional-hazards testing and time-varying analysis, sensitivity analyses, and the time-dependent ROC analysis can be found in the Supplementary Methods. Corresponding detailed results for the complete-case univariate Cox analyses, model-comparison and penalized-regression analyses, continuous-variable and spline analyses, proportional-hazards and time-varying analyses, the time-dependent ROC analysis, and the expanded patient-screening and missing-data assessment are provided in the Supplementary Results.

Variables with univariate p values <0.10 were entered into the adjusted models; several did not converge due to quasi-complete separation in small strata and were excluded. A two-sided $p<0.05$ was considered significant. Descriptive statistics, Kaplan–Meier/log-rank analysis, and the primary Cox models were used with IBM SPSS Statistics v30.0; all sensitivity and robustness analyses were conducted with R 4.6.0 (survival, rms, timeROC, splines packages).

3 | Results

3.1 | Patient Characteristics and Biomarker Availability

Of the 120 patients screened, 5 were excluded for de novo metastatic disease, 17 for no pretreatment PET/CT, and 12 for externally acquired PET/CT whose source DICOM data could not be obtained for standardized quantitative analysis, leaving the 86-patient overall cohort (Figure 1). Of these 86 baseline examinations, 57 (66.3%) were performed in-house and 29 (33.7%) at outside institutions, the latter imported as DICOM data and re-segmented centrally using identical methodology (Section 2). Pretreatment EBV-DNA was available in 66 patients, TLG was reliably quantifiable in 76, and both in 59, who comprised the complete-case cohort. Baseline characteristics are in Table 1. Median age was 49 years (range: 12–76), 77.9% were male, 93.0% had nonkeratinizing undifferentiated histology, and 80.3% presented with Stage III–IVA disease. The 6 "Other" histology cases were 5 keratinizing SCC and 1 nonkeratinizing differentiated carcinoma. Seven patients (8.1%) were aged ≤15 years; they received the same curative-intent dose and fractionation as adults (66–70 Gy) and concurrent chemotherapy at a comparable rate (6/7), not a separate pediatric protocol. VMAT was used in 81.4%, neoadjuvant chemotherapy in 34.9%, and concurrent

10970215, 0, Downloaded from https://onlinelibrary.wiley.com/doi/10.1002/ijc.70732 by Mehmet Çar Duymaz - Dokuz Eylul University , Wiley Online Library on [02/09/2026]. See the Terms and Conditions (https://onlinelibrary.wiley.com/terms-and-conditions) on Wiley Online Library for rules of use; OA articles are governed by the applicable Creative Commons License

TABLE 2 | Cox regression analyses for PFS and OS, combined (complete-case cohort, $n = 59$; exploratory).

Variable	PFS HR	PFS 95% CI	PFS *p*	OS HR	OS 95% CI	OS *p*
Model 1: Individual biomarkers						
EBV-DNA ≥ 3500 copies/mL	3.05	0.92–10.15	0.069	2.69	0.54–13.49	0.229
TLG ≥ 200	2.30	0.74–7.16	0.150	4.81	0.96–24.14	0.056
T3–4 vs. T1–2	2.96	0.95–9.23	0.062	—	—	—
RT duration ≤ 49 days	3.14	0.85–11.62	0.087	—	—	—
Model 2: Composite biomarker						
$EBV\text{-}DNA_{high}/TLG_{high}$ vs. others	3.97	1.32–11.93	0.014	4.13	1.10–15.52	0.036
T3–4 vs. T1–2	3.18	1.03–9.84	0.045	—	—	—
RT duration ≤ 49 days	3.06	0.83–11.32	0.094	—	—	—

Note: HRs for PFS Model 1, PFS Model 2, and OS Model 1 are mutually adjusted within their respective models (i.e., each covariate's HR accounts for the other covariates listed in that model block). OS Model 2 contains the composite variable alone, with no formal adjustment for other covariates; it should be read as an exploratory single-variable association, not an independently adjusted predictor (see Sections 2 and 3). "—" indicates the covariate was not entered in that model (it did not meet the $p < 0.10$ univariate screening threshold for that endpoint). Model fit: PFS Model 1, $\chi^2 = 14.20$, df = 4, $p = 0.007$, apparent/optimism-corrected $C = 0.792/0.738$, AIC = 90.9; PFS Model 2, $\chi^2 = 13.06$, df = 3, $p = 0.005$, apparent/optimism-corrected $C = 0.768/0.726$, AIC = 90.0; OS Model 1, $\chi^2 = 8.02$, df = 2, $p = 0.018$, apparent/optimism-corrected $C = 0.794/0.756$, AIC = 58.1; OS Model 2, $\chi^2 = 4.29$, df = 1, $p = 0.038$, apparent/optimism-corrected $C = 0.675/0.666$, AIC = 59.8. The proportional-hazards assumption held for all four models by Schoenfeld residual testing (all $p > 0.2$; Supplementary Results). Motivated by the visual Kaplan–Meier separation pattern, an exploratory piecewise Cox analysis (Results) descriptively found a stronger composite-variable association with PFS in the first 30 months (HR = 5.14) than beyond (HR = 1.70), despite the absence of a detected proportional-hazards violation. Full penalized (ridge) coefficients for all four models are in Table S5. RT duration ≤ 49 days is the higher-hazard group (see Section 2).

TABLE 3 | Survival outcomes by EBV-DNA/TLG risk group ($n = 59$), with 95% confidence intervals.

Risk group	*n*	PFS events	5-year PFS (%, 95% CI)	OS events	5-year OS (%, 95% CI)
$EBV\text{-}DNA_{low}/TLG_{low}$	24	2	89.7 (64.0–97.4)	0	100.0 (not estimable)
$EBV\text{-}DNA_{high}/TLG_{low}$	13	3	82.5 (46.1–95.3)	2	87.5 (38.7–98.1)
$EBV\text{-}DNA_{low}/TLG_{high}$	10	2	75.0 (31.5–93.1)	2	70.0 (22.5–91.8)
$EBV\text{-}DNA_{high}/TLG_{high}$	12	6	58.3 (27.0–80.1)	5	75.0 (40.8–91.2)
Overall (complete-case)	59	13	—	9	—

Note: Log-rank test: PFS $p = 0.042$; OS $p = 0.044$. $EBV\text{-}DNA_{high}/TLG_{high}$ vs. all others: PFS $p = 0.008$; OS $p = 0.023$ (Figure S1). Event columns report total events over the entire follow-up period ($EBV\text{-}DNA_{high}/TLG_{high}$ group: 5 deaths total, 3 within the first 30 months, 2 more at ~78 and ~82 months). The 5-year % columns are landmark Kaplan–Meier estimates at exactly 60 months, not a simple ratio of the total event count. No deaths were observed in the $EBV\text{-}DNA_{low}/TLG_{low}$ group, so its 5-year OS confidence interval is not estimable; interpret this and the other small-sample Kaplan–Meier tails with caution. The 5-year OS ordering across the four groups is not strictly monotonic ($EBV\text{-}DNA_{low}/TLG_{high}$'s 70.0% is numerically lower than $EBV\text{-}DNA_{high}/TLG_{high}$'s 75.0%), unlike the PFS column, which decreases monotonically; this should not be described as a strict four-tier OS gradient (see Section 4).

chemotherapy in 87.2%. Radiotherapy was interrupted for at least 1 day in 4 patients (4.7%).

Both EBV-DNA and TLG were available in 59/86 patients (68.6%). These patients were stratified into four risk groups: $EBV\text{-}DNA_{low}/TLG_{low}$ ($n = 24$, 40.7%), $EBV\text{-}DNA_{high}/TLG_{low}$ ($n = 13$, 22.0%), $EBV\text{-}DNA_{low}/TLG_{high}$ ($n = 10$, 17.0%), and $EBV\text{-}DNA_{high}/TLG_{high}$ ($n = 12$, 20.3%). Group assignment used the prespecified EBV-DNA cutoff (3500 copies/mL) and the TLG cutoff (200; supported by a same-cohort time-dependent ROC analysis).

3.2 | Survival Outcomes

At a median follow-up of 75.5 months (95% CI: 62.4 months to not reached), 5-year PFS and OS for the entire cohort ($n = 86$) were 81.1% (95% CI: 70.6%–88.2%) and 85.9% (95% CI: 75.2%–92.2%), respectively (20 PFS events: 15 progressions, 5 deaths without documented progression; 16 deaths total, 11 disease-related). Among the nine patients who developed distant metastases, the most common sites were the lung ($n = 5$), bone ($n = 4$), and liver ($n = 3$). These sites are not mutually exclusive: three patients had two involved sites.

3.3 | Univariate and Adjusted Cox Regression (Complete-Case Cohort, $n = 59$)

Univariate results for PFS and OS (13 and 9 events, respectively) are reported in full in Table S2. The strongest univariate predictors for both endpoints were the $EBV\text{-}DNA_{high}/TLG_{high}$ group (PFS HR = 4.01, 95% CI: 1.34–12.01; OS HR = 4.13, 95% CI: 1.10–15.52) and TLG ≥ 200 (PFS HR = 3.29, 95% CI: 1.07–10.08; OS HR = 6.11, 95% CI: 1.26–29.60); EBV-DNA ≥ 3500 copies/mL and T3–4 classification showed weaker associations. Several models (e.g., female sex) did not converge due to quasi-complete separation in small strata.

10970215, 0, Downloaded from https://onlinelibrary.wiley.com/doi/10.1002/ijc.70732 by Mehmet Çar Duymaz - Dokuz Eylul University , Wiley Online Library on [02/09/2026]. See the Terms and Conditions (https://onlinelibrary.wiley.com/terms-and-conditions) on Wiley Online Library for rules of use; OA articles are governed by the applicable Creative Commons License

Two Cox model formulations were fit for each endpoint (Table 2). For PFS, Model 1 (individual biomarkers: TLG, EBV-DNA, T-classification, RT duration) was globally significant ($\chi^2 = 14.20$, $p = 0.007$), but no single covariate reached significance. Model 2 (composite biomarker in place of the individual markers) was likewise globally significant ($\chi^2 = 13.06$, $p = 0.005$), with the composite variable and T-classification both remaining statistically associated with PFS in the adjusted exploratory model. For OS, Model 1 (TLG, EBV-DNA) showed a trend for TLG ($p = 0.056$). Model 2 contained the composite variable alone (the only covariate meeting univariate screening for OS) and was significant (HR = 4.13, $p = 0.036$). Because this model contains only one variable, the OS result is an unadjusted association, not an independently adjusted predictor.

Nonnested model comparison (apparent/optimism-corrected C-index, AIC; Supplementary Methods) showed the composite model discriminated comparably to, but not better than, the individual-biomarker model for PFS (corrected $C = 0.726$ vs. 0.738), and less well for OS (corrected $C = 0.666$ vs. 0.756). Penalized (ridge) regression with a fixed, modest penalty produced concordant but attenuated estimates for all four models (full coefficients in Table S5). The association of the composite variable remained significant for PFS (ridge $p = 0.017$) and nominally significant for OS (ridge $p = 0.042$), while the individual-biomarker covariates no longer reached significance. Penalization does not eliminate overfitting, and the attenuation, with the small event counts, calls for caution.

Schoenfeld residual testing showed the proportional-hazards assumption held for all four models, including the composite variable in PFS Model 2 ($p = 0.26$) and OS Model 2 ($p = 0.75$; full results in Supplementary Results). Motivated by the visual separation in the Kaplan–Meier curves rather than by a test result, we performed a post hoc piecewise Cox analysis split at 30 months. For the composite variable and PFS, the HR was 5.14 (95% CI: 1.48–17.80, $p = 0.010$) for months 0–30 and 1.70 (95% CI: 0.15–19.00, $p = 0.667$) beyond 30 months. A covariate-by-log(time) interaction term was consistent in direction but nonsignificant ($p = 0.186$), likely reflecting limited events. Because the proportional-hazards test detected no violation, this is descriptive and does not confirm a time-varying hazard. An analogous OS check showed no significant early/late difference.

Continuous and natural-cubic-spline models (Supplementary Methods) showed continuous TLG remained associated with OS (per-100-unit HR = 1.23, 95% CI: 1.02–1.49, $p = 0.028$), with a nonsignificant PFS trend ($p = 0.072$). Log-EBV-DNA was not significant when modeled linearly for either endpoint, unlike its dichotomized, borderline-significant form, a threshold-sensitivity discussed in Limitations. Splines detected no evidence of nonlinearity for TLG ($p = 0.85$ PFS, $p = 0.62$ OS), which does not establish linearity and does not validate the TLG = 200 threshold. For log-EBV-DNA, splines showed nonlinearity for PFS ($p = 0.036$) and a borderline signal for OS ($p = 0.073$), suggesting neither the linear nor the dichotomized (3500 copies/mL) form captures its dose–response well. Given the small available-case sample ($n = 66$, 15 PFS events), this needs cautious interpretation (Limitations).

The VMAT-only and pediatric-exclusion sensitivity analyses (Table S6), both restricted to the composite biomarker, left this association materially unchanged. In the available-case sensitivity analyses, which examined the individual biomarkers rather than the composite (Tables S3 and S4), TLG ≥ 200 remained significantly associated with both endpoints, while EBV-DNA ≥ 3500 copies/mL did not.

Because baseline imaging was not acquired on a single scanner, we performed a post hoc robustness analysis restricted to the 57 patients whose baseline PET/CT was performed in-house (Table S7). Among the 50 with quantifiable TLG (12 PFS and 11 OS events), TLG ≥ 200 remained associated with inferior PFS (HR = 4.37, 95% CI: 1.18–16.19; $p = 0.027$) and OS (HR = 6.56, 95% CI: 1.41–30.49; $p = 0.016$). Continuous TLG was also associated with both endpoints (PFS per-100-unit HR = 1.22, 95% CI: 1.01–1.48, $p = 0.037$; OS HR = 1.26, 95% CI: 1.04–1.53, $p = 0.020$). The re-estimated Youden-optimal cut-point was nearly identical to the full-cohort value (196.8 vs. 196.5). In the smaller in-house complete-case cohort ($n = 34$; 7 PFS and 6 OS events), the adjusted composite association with PFS was of borderline significance (Model 2 HR 4.81, 95% CI: 1.00–23.08, $p = 0.050$, vs. 3.97 in the full complete-case cohort). The piecewise 0–30-month PFS estimate was HR 4.97, 95% CI: 0.83–29.82, $p = 0.079$, versus 5.14 in the full cohort. Confidence intervals widened, however, and precision fell. The four-group log-rank comparison no longer reached significance for PFS ($p = 0.169$) or OS ($p = 0.074$), and the ordering was no longer monotonic (5-year PFS 90.9%, 100%, 66.7%, and 66.7% for Groups 1–4). The binary EBV-DNA$_{high}$/TLG$_{high}$ comparison remained significant for both endpoints (PFS $p = 0.034$; OS $p = 0.018$), while continuous log-transformed EBV-DNA showed essentially no association (PFS HR = 0.99, 95% CI: 0.80–1.23, $p = 0.94$). These patterns are compatible with reduced precision after restriction to a smaller subgroup. Residual effect heterogeneity cannot be excluded. Because the subgroup comes from within the primary cohort and the TLG cut-point was re-optimized in it, this is an internal robustness analysis, not independent validation.

3.4 | Risk Stratification by Combined EBV-DNA/TLG Groups

Across the four groups in the complete-case cohort ($n = 59$), Kaplan–Meier curves separated significantly for both PFS (log-rank $p = 0.042$) and OS (log-rank $p = 0.044$) (Table 3; Figure 2). Five-year PFS decreased monotonically across groups: 89.7% (95% CI: 64.0%–97.4%) for EBV-DNA$_{low}$/TLG$_{low}$, 82.5% for EBV-DNA$_{high}$/TLG$_{low}$, 75.0% for EBV-DNA$_{low}$/TLG$_{high}$, and 58.3% (95% CI: 27.0%–80.1%) for EBV-DNA$_{high}$/TLG$_{high}$ (the lowest of the four).

For OS, EBV-DNA$_{low}$/TLG$_{low}$ had no deaths (100% 5-year OS), EBV-DNA$_{high}$/TLG$_{low}$ and EBV-DNA$_{low}$/TLG$_{high}$ had 87.5% and 70.0%, and EBV-DNA$_{high}$/TLG$_{high}$ had 75.0% (95% CI: 40.8%–91.2%). The value for EBV-DNA$_{high}$/TLG$_{high}$ is numerically similar to, not lower than, EBV-DNA$_{low}$/TLG$_{high}$'s 70.0%, so the four-group OS ordering is not strictly monotonic (unlike PFS) and should not be described as a strict gradient (Table 3). EBV-DNA$_{high}$/TLG$_{high}$ had the most total deaths (5/12), and its OS estimate fell to 45.0% at approximately 8.7 years of follow-up,

10970215, 0, Downloaded from https://onlinelibrary.wiley.com/doi/10.1002/ijc.70732 by Mehmet Çar Duymaz - Dokuz Eylul University , Wiley Online Library on [02/09/2026]. See the Terms and Conditions (https://onlinelibrary.wiley.com/terms-and-conditions) on Wiley Online Library for rules of use; OA articles are governed by the applicable Creative Commons License

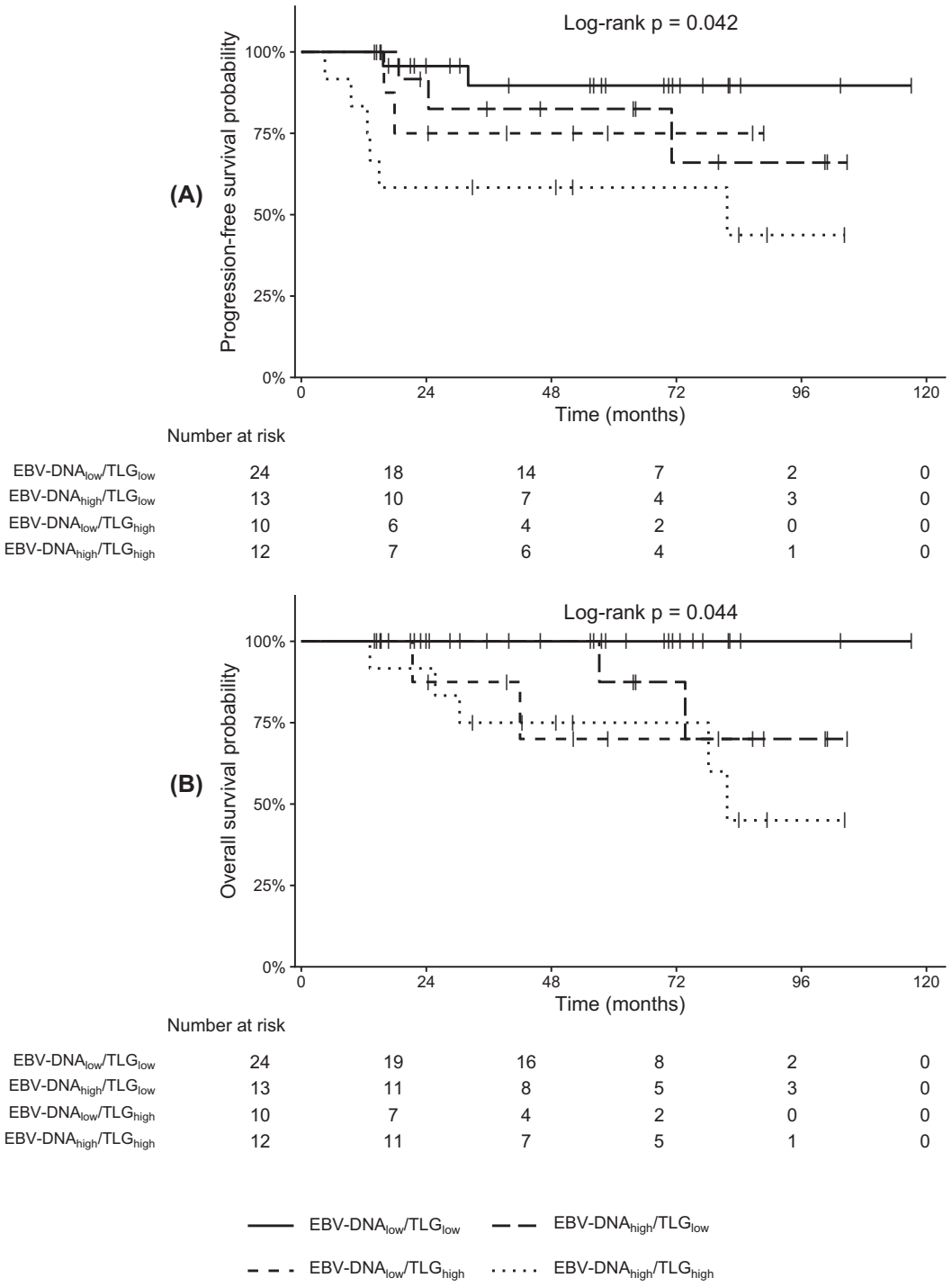

FIGURE 2 | Kaplan–Meier curves for the four-tier EBV-DNA/TLG risk stratification in the complete-case cohort ($n = 59$). (A) Progression-free survival by risk group (EBV-DNA$_{low}$/TLG$_{low}$, EBV-DNA$_{high}$/TLG$_{low}$, EBV-DNA$_{low}$/TLG$_{high}$, EBV-DNA$_{high}$/TLG$_{high}$; log-rank $p = 0.042$). (B) Overall survival by risk group (log-rank $p = 0.044$). Numbers-at-risk tables are shown below each panel; 95% confidence intervals for 5-year estimates are reported in Table 3. See Figure S1 for the binary EBV-DNA$_{high}$/TLG$_{high}$-vs.-others comparison.

after two further deaths at approximately 78 and 82 months (Figure 2). Three of its five deaths occurred within the first 30 months. This pattern is descriptive, because the analogous piecewise check for OS was not statistically significant. A binary comparison (EBV-DNA$_{high}$/TLG$_{high}$ vs. all others) showed consistent separation for both endpoints (PFS log-rank $p = 0.008$; OS $p = 0.023$; Figure S1).

4 | Discussion

Among the 59 complete-case patients drawn from an eligible cohort of 86 nonmetastatic NPC patients in a nonendemic region, composite EBV-DNA/TLG risk stratification was associated with both PFS and OS. The EBV-DNA$_{high}$/TLG$_{high}$ subgroup had a nearly fourfold higher hazard of progression (adjusted

10970215, 0, Downloaded from https://onlinelibrary.wiley.com/doi/10.1002/ijc.70732 by Mehmet Çar Duymaz - Dokuz Eylul University , Wiley Online Library on [02/09/2026]. See the Terms and Conditions (https://onlinelibrary.wiley.com/terms-and-conditions) on Wiley Online Library for rules of use; OA articles are governed by the applicable Creative Commons License

HR = 3.97) and, in a single-variable model, of death (HR = 4.13). These findings are consistent with EBV-DNA and TLG reflecting partly overlapping aspects of disease burden [12, 14, 15, 22, 23]. Model comparison, however, did not show the composite outperforming the individual biomarkers: discrimination was comparable for PFS and lower for OS.

The EBV-DNA effect seen here is broadly consistent with meta-analytic evidence from endemic populations (pooled HR > 2.0 [16, 17]), but it did not reach significance after adjustment (adjusted HR = 3.05, $p = 0.069$) or when modeled continuously, likely reflecting both limited power and threshold-sensitivity. Confidence in the specific 3500 copies/mL cutoff should therefore remain low [13]. TLG was the strongest univariate OS predictor and remained associated with OS continuously, consistent with meta-analytic pooled HRs of 2.6–3.3 [22, 24]. When co-entered with EBV-DNA, the dichotomized TLG association with OS fell short of significance (adjusted HR = 4.81, 95% CI: 0.96–24.14, $p = 0.056$); the corresponding PFS estimate, additionally adjusted for T classification and radiotherapy duration, was also nonsignificant (adjusted HR = 2.30, 95% CI: 0.74–7.16, $p = 0.150$). This likely reflects overlapping disease-burden information, as Chang et al. also reported ($R^2 = 0.589$ between TLG and EBV-DNA) [26]. Because the two markers are correlated, a composite category avoids entering them as correlated continuous markers in a single model. That is a statistical rather than a biological justification, and it did not yield superior OS discrimination.

The four-tier Kaplan–Meier gradient for PFS, together with the stronger early PFS association seen in the piecewise Cox analysis, is consistent with worse outcomes when both markers are high [12, 14, 15, 22, 23]. The early deaths observed in the highest-risk group are a descriptive observation from the Kaplan–Meier curves rather than a separately confirmed statistical finding. For OS, however, this gradient was not strictly monotonic across all four groups, and estimates carried wide, overlapping confidence intervals given small subgroup sizes ($n = 10$–24). The OS interpretation should therefore remain cautious. Our results extend prior work on EBV-DNA and PET-derived volumetric biomarkers in NPC [26, 28–31] by testing a simple, binary EBV-DNA/TLG composite in the curative nonmetastatic setting. Incremental value over the individual markers is still unproven.

Whether this classification can inform treatment selection should be tested prospectively [32–34]. No treatment modification is supported by the present data.

A strength of this study is the nonendemic setting: Türkiye has markedly lower age-standardized NPC incidence than Southern China and Southeast Asia, where most EBV-DNA-guided risk-stratification literature originates [1–3, 5]. In this cohort, with nonkeratinizing undifferentiated histology (93.0%), male predominance (77.9%), and mostly locoregionally advanced disease (80.3% Stage III–IVA), TLG showed the clearest individual association, whereas the incremental contribution of EBV-DNA remained uncertain. These findings demonstrate feasibility in a nonendemic setting but do not establish geographic external validity [35, 36]. The thresholds used require external, prospective validation.

4.1 | Limitations

This study has several limitations. Its retrospective, single-center design is susceptible to selection and information bias. Although cohort-level reasons for missing PET/CT data and nonquantifiable TLG were documented, patient-specific reasons for missing EBV-DNA could not be reconstructed; therefore, EBV-DNA missingness cannot be assumed to be random. Complete-case and noncomplete-case patients also differed in nodal stage, overall stage, and RT technique (Table S1). A VMAT-only sensitivity analysis yielded similar results but cannot eliminate this potential selection bias.

The modest sample size ($n = 86$ overall; $n = 59$ complete-case) and limited events (13 PFS and 9 OS) constrained model complexity and stability, leading to nonconvergence due to quasi-complete separation in several small strata. Accordingly, all Cox-model findings are exploratory. Penalized regression and bootstrap validation can characterize, but cannot eliminate, overfitting or substitute for external validation.

The TLG = 200 threshold was derived and evaluated in the same cohort; the similar time-dependent ROC cut-point of 195.9 came from the same cohort and is not independent validation. Moreover, 29 of 86 PET/CT examinations were acquired externally, without cross-scanner harmonization. Relative-threshold segmentation and central re-segmentation by one reader may have reduced but cannot eliminate acquisition-related variability. The in-house robustness analysis ($n = 57$; Table S7) produced directionally similar estimates, with significant individual TLG associations, although the adjusted PFS association for the composite marker was only of borderline significance; precision decreased substantially in the smaller complete-case subgroup ($n = 34$; 7 PFS and 6 OS events). Inter-observer reproducibility was not assessed. For equivocal nodes without histopathological confirmation, classification was based on the assessment of the single reader. Imaging and treatment practices may also have evolved during the 14-year study period.

Additional treatment-related confounding is possible. Concurrent chemotherapy schedule and cumulative cisplatin dose could not be reliably reconstructed; chemotherapy dose reductions and omitted cycles were not systematically documented. Radiotherapy interruptions occurred in four patients, but duration was available for only three. Preanalytic EBV-DNA storage duration was also unavailable.

Seven patients were aged ≤ 15 years, including three complete-case patients. Their exclusion did not materially change the composite-biomarker findings (Table S6), although this subgroup was small. The counterintuitive, nonsignificant association between shorter RT duration and worse outcomes (PFS $p = 0.068$; OS $p = 0.219$) may reflect chance or residual confounding and should not support clinical inference.

Finally, continuous EBV-DNA showed weaker associations than its dichotomized form, while spline analysis suggested nonlinearity for PFS ($p = 0.036$); continuous log-EBV-DNA was not associated with either endpoint in the in-house analysis (PFS HR = 0.99, $p = 0.94$). This nonlinearity appears to be driven by the eight

10970215, 0, Downloaded from https://onlinelibrary.wiley.com/doi/10.1002/ijc.70732 by Mehmet Çar Duymaz - Dokuz Eylul University , Wiley Online Library on [02/09/2026]. See the Terms and Conditions (https://onlinelibrary.wiley.com/terms-and-conditions) on Wiley Online Library for rules of use; OA articles are governed by the applicable Creative Commons License

patients with undetectable EBV-DNA rather than by a graded effect among patients with measurable virus: excluding them, the spline test no longer indicates departure from linearity (PFS $p = 0.19$, OS $p = 0.25$). Four of these eight had keratinizing squamous cell carcinoma, four of the five keratinizing cases in the entire cohort, so undetectable EBV-DNA in this nonendemic series may mark a biologically distinct, largely EBV-unrelated subgroup rather than the low end of a continuum. Their outcomes were numerically worse than those of patients with detectable virus, but the difference was not statistically significant (PFS HR = 1.83, 95% CI: 0.52–6.50; OS HR = 3.27, 95% CI: 0.87–12.36); with eight patients and three events this remains a hypothesis for larger series to test. The composite category is therefore threshold-sensitive and hypothesis-generating, and is not evidence of an independent or synergistic EBV-DNA effect. Larger prospective studies with prespecified thresholds are needed.

4.2 | Future Directions and Conclusion

The next step is external, multicenter validation with standardized EBV-DNA and PET protocols, adequate event counts, and preregistered analysis plans, ideally alongside additional biomarkers (radiomics, inflammatory indices) [18, 29].

In conclusion, a pretreatment composite EBV-DNA (≥3500 copies/mL)/TLG (≥200) stratification identified an $EBV\text{-}DNA_{high}$/TLG_{high} subgroup with inferior PFS and OS, with discrimination comparable to the individual biomarkers for PFS and lower for OS. Given the small sample, limited events, and absence of independent validation, this model is hypothesis-generating rather than clinically actionable and needs prospective, multicenter validation.

Author Contributions

Mehmet Çağrı Duymaz: conceptualization, investigation, writing – original draft, writing – review and editing, visualization, validation, methodology, data curation, resources. **Ece Özkaya Duymaz:** conceptualization, investigation, writing – original draft, methodology, validation, visualization, writing – review and editing, data curation, resources. **Nazlı Ünsal:** conceptualization, investigation, writing – original draft, formal analysis, methodology, validation, writing – review and editing, data curation, resources. **Recep Bekiş:** conceptualization, writing – review and editing, methodology, software, supervision. **Büşra Tozduman:** methodology, formal analysis, project administration, writing – original draft, writing – review and editing. **Özgür Appak:** validation, writing – review and editing, resources. **Ayşe Demiral:** writing – review and editing, writing – original draft, visualization, supervision. **Oğuz Çetinayak:** writing – review and editing, validation, methodology, software, formal analysis, project administration, visualization, supervision.

Acknowledgments

AI-assisted tools (ChatGPT v5.2) were used solely for English language refinement. The graphical abstract was created in BioRender. Duymaz, M. Ç. (2026) https://BioRender.com/una8s98.

Ethics Statement

This study was approved by the Non-Interventional Research Ethics Committee of Dokuz Eylül University (approval no: 2026/02-12) and was conducted in accordance with the Declaration of Helsinki. The ethics committee waived the requirement for informed consent due to the retrospective design and the use of de-identified patient data.

Conflicts of Interest

The authors declare no conflicts of interest.

Data Availability Statement

Individual-level patient data is protected by institutional ethics regulations. The de-identified datasets can be found on Figshare (https://doi.org/10.6084/m9.figshare.33174539). All source code is publicly available on GitHub (https://github.com/mehmetduymaz4-cpu/npc-ebv-tlg-risk-stratification). Further information is available from the corresponding author upon request.

References

1. Y. P. Chen, A. T. C. Chan, Q. T. Le, P. Blanchard, Y. Sun, and J. Ma, "Nasopharyngeal Carcinoma," *Lancet* 394, no. 10192 (2019): 64–80.

2. Z. Y. Su, P. Y. Siak, Y. Y. Lwin, and S. C. Cheah, "Epidemiology of Nasopharyngeal Carcinoma: Current Insights and Future Outlook," *Cancer Metastasis Reviews* 43, no. 3 (2024): 919–939.

3. F. Bray, M. Laversanne, H. Sung, et al., "Global Cancer Statistics 2022: GLOBOCAN Estimates of Incidence and Mortality Worldwide for 36 Cancers in 185 Countries," *CA: A Cancer Journal for Clinicians* 74, no. 3 (2024): 229–263.

4. Q. Liu, H. Wang, Z. Chen, et al., "Global, Regional, and National Epidemiology of Nasopharyngeal Carcinoma in Middle-Aged and Elderly Patients From 1990 to 2021," *Ageing Research Reviews* 104 (2025): 102613.

5. E. T. Chang, W. Ye, Y. X. Zeng, and H. O. Adami, "The Evolving Epidemiology of Nasopharyngeal Carcinoma," *Cancer Epidemiology, Biomarkers and Prevention* 30, no. 6 (2021): 1035–1047.

6. K. C. W. Wong, E. P. Hui, K. W. Lo, et al., "Nasopharyngeal Carcinoma: An Evolving Paradigm," *Nature Reviews. Clinical Oncology* 18, no. 11 (2021): 679–695.

7. P. Blanchard, A. Lee, S. Marguet, et al., "Chemotherapy and Radiotherapy in Nasopharyngeal Carcinoma: An Update of the MAC-NPC Meta-Analysis," *Lancet Oncology* 16, no. 6 (2015): 645–655.

8. Y. Li, Z. Huang, X. Zeng, et al., "Early Recurrence as a Pivotal Event in Nasopharyngeal Carcinoma: Identifying Predictors and Key Molecular Signals for Survivors," *Head and Face Medicine* 20 (2024): 55.

9. M. B. Amin, S. B. Edge, F. L. Greene, et al., eds., *AJCC Cancer Staging Manual*, 8th ed. (Springer, 2017).

10. F. P. Chen, L. Lin, J. Liang, et al., "Development of a Risk Classification System Combining TN-Categories and Circulating EBV DNA for Non-Metastatic NPC in 10,149 Endemic Cases," *Therapeutic Advances in Medical Oncology* 13 (2021): 17588359211052417.

11. W. Z. Li, H. J. Wu, S. H. Lv, et al., "Assessment of Survival Model Performance Following Inclusion of Epstein-Barr Virus DNA Status in Conventional TNM Staging Groups in Epstein-Barr Virus-Related Nasopharyngeal Carcinoma," *JAMA Network Open* 4, no. 9 (2021): e2124721.

12. Y. M. D. Lo, A. T. C. Chan, L. Y. S. Chan, et al., "Molecular Prognostication of Nasopharyngeal Carcinoma by Quantitative Analysis of Circulating Epstein-Barr Virus DNA," *Cancer Research* 60, no. 24 (2000): 6878–6881.

13. A. W. M. Lee, V. H. F. Lee, W. T. Ng, et al., "A Systematic Review and Recommendations on the Use of Plasma EBV DNA for Nasopharyngeal Carcinoma," *European Journal of Cancer* 153 (2021): 109–122.

14. S. F. Leung, B. Zee, B. B. Y. Ma, et al., "Plasma Epstein-Barr Viral Deoxyribonucleic Acid Quantitation Complements Tumor-Node-Metastasis Staging Prognostication in Nasopharyngeal Carcinoma," *Journal of Clinical Oncology* 24, no. 34 (2006): 5414–5418.

15. L. Peng, Y. Yang, R. Guo, et al., "Relationship Between Pretreatment Concentration of Plasma Epstein-Barr Virus DNA and Tumor Burden

10970215, 0, Downloaded from https://onlinelibrary.wiley.com/doi/10.1002/ijc.70732 by Mehmet Çar Duymaz - Dokuz Eylul University , Wiley Online Library on [02/09/2026]. See the Terms and Conditions (https://onlinelibrary.wiley.com/terms-and-conditions) on Wiley Online Library for rules of use; OA articles are governed by the applicable Creative Commons License

in Nasopharyngeal Carcinoma: An Updated Interpretation," *Cancer Medicine* 7, no. 12 (2018): 5988–5998.

16. H. Qu, Y. Huang, S. Zhao, Y. Zhou, and W. Lv, "Prognostic Value of Epstein-Barr Virus DNA Level for Nasopharyngeal Carcinoma: A Meta-Analysis of 8128 Cases," *European Archives of Oto-Rhino-Laryngology* 277, no. 1 (2020): 9–18.

17. I. El Alami, A. Gihbid, H. Charoute, et al., "Prognostic Value of Epstein-Barr Virus DNA Load in Nasopharyngeal Carcinoma: A Meta-Analysis," *Pan African Medical Journal* 41 (2022): 6.

18. H. T. Hsieh, X. Y. Zhang, Y. Wang, and X. Q. Cheng, "Biomarkers for Nasopharyngeal Carcinoma," *Clinica Chimica Acta* 572 (2025): 120257.

19. S. M. Larson, Y. Erdi, T. Akhurst, et al., "Tumor Treatment Response Based on Visual and Quantitative Changes in Global Tumor Glycolysis Using PET-FDG Imaging: The Visual Response Score and the Change in Total Lesion Glycolysis," *Clinical Positron Imaging* 2, no. 3 (1999): 159–171.

20. S. S. Yang, Y. S. Wu, W. C. Chen, et al., "Benefit of [18F]-FDG PET/CT for Treatment-Naïve Nasopharyngeal Carcinoma," *European Journal of Nuclear Medicine and Molecular Imaging* 49, no. 3 (2022): 980–991.

21. J. Yoo, S. Henderson, and C. Walker-Dilks, "Evidence-Based Guideline Recommendations on the Use of Positron Emission Tomography Imaging in Head and Neck Cancer," *Clinical Oncology (Royal College of Radiologists)* 25, no. 4 (2013): e33–e66.

22. Q. Li, J. Zhang, W. Cheng, et al., "Prognostic Value of Maximum Standard Uptake Value, Metabolic Tumor Volume, and Total Lesion Glycolysis of Positron Emission Tomography/Computed Tomography in Patients With Nasopharyngeal Carcinoma: A Systematic Review and Meta-Analysis," *Medicine (Baltimore)* 96, no. 37 (2017): e8084.

23. S. H. Moon, J. Y. Choi, H. J. Lee, et al., "Prognostic Value of Volume-Based Positron Emission Tomography/Computed Tomography in Patients With Nasopharyngeal Carcinoma Treated With Concurrent Chemoradiotherapy," *Clinical and Experimental Otorhinolaryngology* 8, no. 2 (2015): 142–148.

24. K. Pak, G. J. Cheon, H. Y. Nam, et al., "Prognostic Value of Metabolic Tumor Volume and Total Lesion Glycolysis in Head and Neck Cancer: A Systematic Review and Meta-Analysis," *Journal of Nuclear Medicine* 55, no. 6 (2014): 884–890.

25. B. Gu, J. Zhang, G. Ma, et al., "Establishment and Validation of a Nomogram With Intratumoral Heterogeneity Derived From ^{18}F-FDG PET/CT for Predicting Individual Conditional Risk of 5-Year Recurrence Before Initial Treatment of Nasopharyngeal Carcinoma," *BMC Cancer* 20, no. 1 (2020): 37.

26. K. P. Chang, N. M. Tsang, C. T. Liao, et al., "Prognostic Significance of ^{18}F-FDG PET Parameters and Plasma Epstein-Barr Virus DNA Load in Patients With Nasopharyngeal Carcinoma," *Journal of Nuclear Medicine* 53, no. 1 (2012): 21–28.

27. B. B. Ma, F. K. Mo, A. T. C. Chan, et al., "The Prognostic Significance of Tumor Vascular Invasion and Its Association With Plasma Epstein-Barr Virus DNA, Tumor Volume and Metabolic Activity in Locoregionally Advanced Nasopharyngeal Carcinoma," *Oral Oncology* 44, no. 11 (2008): 1067–1072.

28. X. Zhou, Y. Yang, X. Ou, T. Xu, C. Shen, and C. Hu, "Interplay of Tumor Spread, Volume and Epstein-Barr Virus DNA in Nasopharyngeal Carcinoma: Feasibility of an Integrative Risk Stratification Scheme," *Journal of Cancer* 9, no. 22 (2018): 4271–4278.

29. J. Zhou, Y. Hua, C. Zhang, et al., "Multimodal Glyco-Lipid-EBVDNA Signature Prognostic Model for Individualized Risk Stratification of Locally Advanced Nasopharyngeal Carcinoma," *European Journal of Nuclear Medicine and Molecular Imaging* 53 (2026): 4460–4476, https://doi.org/10.1007/s00259-026-07781-x.

30. S. C. Chan, C. L. Hsu, T. C. Yen, S. H. Ng, C. T. Liao, and H. M. Wang, "The Role of ^{18}F-FDG PET/CT Metabolic Tumour Volume in Predicting Survival in Patients With Metastatic Nasopharyngeal Carcinoma," *Oral Oncology* 49, no. 1 (2013): 71–78.

31. Y. H. Chen, K. P. Chang, S. C. Chu, et al., "Value of Early Evaluation of Treatment Response Using ^{18}F-FDG PET/CT Parameters and the Epstein-Barr Virus DNA Load for Prediction of Outcome in Patients With Primary Nasopharyngeal Carcinoma," *European Journal of Nuclear Medicine and Molecular Imaging* 46, no. 3 (2019): 650–660.

32. X. Liu, Y. Zhang, K. Y. Yang, et al., "Induction-Concurrent Chemoradiotherapy With or Without Sintilimab in Patients With Locoregionally Advanced Nasopharyngeal Carcinoma in China (CONTINUUM): A Multicentre, Open-Label, Parallel-Group, Randomised, Controlled, Phase 3 Trial," *Lancet* 403, no. 10445 (2024): 2720–2731.

33. Y. Liu, Z. Du, S. Song, and J. Yi, "Progress in the Comprehensive Treatment of Nasopharyngeal Carcinoma: A Review for Risk-Stratified Management Strategies," *Holistic Integrative Oncology* 2 (2023): 19.

34. P. Blanchard, F. De Felice, M. L. K. Chua, et al., "Advances in Individualization of Systemic Treatment for Locoregionally Advanced Nasopharyngeal Carcinoma: A Systematic Review," *ESMO Open* 10, no. 4 (2025): 104513.

35. S. Alfieri, R. Romanò, S. Marceglia, et al., "Longitudinal Assessment of Plasma EBV-DNA in Non-Endemic EBV-Related Nasopharyngeal Cancer (NPC): The LEA Study," *European Journal of Cancer* 226 (2025): 115625.

36. R. Pramanik, S. Arora, P. Sharma, et al., "Cell-Free EBV DNA as a Biomarker During Clinical Management of Nasopharyngeal Carcinoma in a Nonendemic Region," *Journal of Medical Virology* 94, no. 2 (2022): 720–728.

Supporting Information

Additional supporting information can be found online in the Supporting Information section. **Table S1:** Comparison of complete-case and noncomplete-case patients. **Table S2:** Univariate Cox regression analysis for PFS and OS (complete-case cohort, $n = 59$; exploratory) Referenced from main text Results and Table 1. Unless otherwise noted, reference categories are the lower-risk/lower-value category shown second in each comparison (e.g., "T3–4 vs. T1–2" has T1–2 as reference). **Table S3:** Sensitivity analysis: univariate Cox regression for PFS using available-case populations. **Table S4:** Sensitivity analysis: univariate Cox regression for OS using available-case populations. **Table S5:** Penalized (ridge) Cox regression: full results for all four Cox models (complete-case cohort, $n = 59$). **Table S6:** Sensitivity analyses: VMAT-only cohort and exclusion of patients aged ≤ 15 years (composite biomarker, complete-case cohort). **Table S7:** Post hoc robustness analysis restricted to patients whose baseline PET/CT was performed in-house Panel A. Individual biomarker analyses—in-house available-case populations. **Figure S1:** Kaplan–Meier curves comparing the EBV-DNAhigh/TLGhigh subgroup versus all other patients in the complete-case cohort ($n = 59$). (A) Progression-free survival (log-rank $p = 0.008$). (B) Overall survival (log-rank $p = 0.023$). Numbers-at-risk tables are shown below each panel.

10970215, 0, Downloaded from https://onlinelibrary.wiley.com/doi/10.1002/ijc.70732 by Mehmet Çar Duymaz - Dokuz Eylul University , Wiley Online Library on [02/09/2026]. See the Terms and Conditions (https://onlinelibrary.wiley.com/terms-and-conditions) on Wiley Online Library for rules of use; OA articles are governed by the applicable Creative Commons License